

Electromagnetic Simulation for THz Antenna-Coupled Microbolometers Operated at Room Temperature

Makoto Aoki, Masanori Takeda, and Norihisa Hiromoto *

Graduate School of Science and Technology, Shizuoka University, 3-5-1 Johoku, Naka-ku,
Hamamatsu 432-8011, Japan

*E-mail: dnhirom@ipc.shizuoka.ac.jp

Abstract

Room-temperature terahertz (THz) detectors with higher performance are necessary for utilizing the THz wave in various sensing, spectroscopy and imaging, but even the best ones in the present are still insufficient for the practical applications. This issue is essential especially in the region around 1 THz at which there exists a large technology gap between microwave and middle-infrared. Therefore, we study to develop an antenna-coupled microbolometer to achieve a high-performance THz detector operated at a room-temperature for sensing at around 1 THz frequency wave. In this paper, we present several important features and results obtained from electromagnetic simulations, which help to design a structure of the antenna and heater to absorb efficiently the power of THz wave.

Abstrak

Simulasi Elektromagnetik terhadap Mikrobolometer Berantena THz Ganda untuk Pengoperasian pada Suhu Ruang. Detektor terahertz (THz) bersuhu ruangan berkinerja tinggi diperlukan untuk memanfaatkan gelombang THz di dalam berbagai proses penangkapan sinyal, spektroskopi, dan penampikan gambar. Namun, detektor terbaik yang ada sekarang pun masih kurang memadai untuk penggunaan praktis. Kekurangan ini menjadi penting, terutama pada daerah sekitar 1 THz di mana terdapat kesenjangan teknologi yang besar antara gelombang mikro dan inframerah-sedang. Oleh karena itu, kami mengadakan penelitian untuk mengembangkan mikrobolometer berantena ganda untuk menghasilkan detektor THz berkinerja tinggi yang dapat dioperasikan pada suhu ruangan untuk menangkap sinyal pada frekuensi gelombang 1 THz. Di dalam makalah ini, kami menyajikan sejumlah fitur dan hasil penting yang didapat dari simulasi elektromagnetik yang dapat membantu dalam merancang struktur antena dan pemanas sehingga mampu menyerap daya gelombang THz secara efisien.

Keywords: detector, dipole antenna, electromagnetic simulation, microbolometer, terahertz (THz)

1. Introduction

Terahertz (THz) technology has rapidly grown after the early innovative study on the THz time-domain spectroscopy in 1990's (e.g. [1-2]) and the invention and improvement of the THz quantum cascade laser in 2000's [3-4]. Various demonstrations for application of THz spectroscopy and imaging have been made so far, such as non-destructive inspection of concealed weapons [5], explosives [6-7] and illegal drugs [8] for security and crime prevention, examination of defects and foreign objects in pharmaceutical tablets[9] and foods [10], diagnosis of tumors [11], analysis of DNA molecules [12], and so on. However, those researches have shown the potential of THz technology, but they have also made the critical issue clear: The present ability of THz technology is still far from demands of

actual use in the field like airports, hospitals, factories etc. That is, the overall performance on sensitivity and speed of measurements is poor and the cost of devices necessary for marginal system is very expensive.

Farther research and development of the sources, detectors, optical elements and measuring techniques as well as sensing systems are crucial for extending the utilization of THz waves. Among a lot of issues, we studies THz detectors and detection systems which have high performance in sensitivity and responding speed, convenience in handling and prospective low-cost after development.

It is necessary for the THz detectors with high detectivity to be cooled down to at least around a liquid helium temperature, whereas the best THz detectors

operated at a room temperature have much worse detectivity by more than four orders in comparison with the cooled THz detectors. The examples of widely-used cooled THz detectors are a composite bolometer [13] and Ge:Ga [14-15] and stressed Ge:Ga photoconductors [16-17], which have noise equivalent power (NEP) of the order of 10^{-14} W/Hz^{1/2} or better values at about 4 K. The main drawback to them is the mandatory use of liquid helium which is troublesome to deal with, needs high cost and has concern about future supply.

To solve the above problems partially, we have made a 4K-cryocooled THz photoconductor system which enables to obtain high-detectivity and rapid-response in THz detection operated without liquid helium. We have demonstrated THz passive imaging of room-temperature objects and evaluated THz emissivity of the material at background-limited performance by the stressed Ge:Ga photoconductor cooled at 4K using a GM mechanical refrigerator [18].

Antenna-coupled detectors have advantage in absorbing THz power at lower frequencies in THz region. A Bi-microbolometer coupled with an antenna has been studied from 1980s [19], and a slot-antenna coupled GaAs Schottky-barrier diode has been developed in millimeter-wave region aiming THz detectors [20]. Recently, an array of antenna-coupled microbolometers with a-Si thermistors is fabricated [21], which NEP still remains in the level of 3×10^{-11} W at 2.4 THz in frequency.

Our research target is to make antenna-coupled THz microbolometers and their array on a Si substrate by MOS technology and to achieve high detectivity and fast response for THz wave at around 1 THz in the room-temperature operation. In this paper, we describe a structure of a microbolometer coupled with a half-wave antenna on a Si substrate and execute the electromagnetic simulation for the model to examine the antenna pattern, antenna currents induced by THz irradiation, and the resonance frequency.

2. Methods

Bolometric-type detectors measure the temperature change caused by absorbing electromagnetic waves as thermal energy. The uncooled microbolometer arrays fabricated using Si technology have been developed in the infrared (IR) region [22-23], which have obtained good sensitivity by a film of the absorption and thermistor layer suspended on the air gap. These infrared bolometer works in the THz region too, if the optics transmits and the irradiated film absorbs the THz waves. However, the THz detector need the larger size than the infrared one due to diffraction. For an example, because the effective refractive index n_e at the surface of a semi-infinite substrate is $n_e = \sqrt{(1 + \epsilon')/2}$, where ϵ' is a relative dielectric constant of the substrate [36],

detector size should be about λ/n_e for the electromagnetic wave of wavelength λ . This size is 119 μm for Si substrate of $\epsilon' = 11.669$ and at 1 THz frequency (300 μm wavelength). It is difficult to fabricate such a large size of the absorption/thermistor film suspended on the air gap and to reduce the thermal capacitance and conductance.

We have proposed a novel structure for the THz microbolometer by adopting an antenna-coupled type to resolve the problem in the microbolometer with surface absorption [24].

The design of the THz antenna-coupled microbolometer is shown in Figs. 1 and 2. The metal antenna is made on the insulation layer of SiO₂ formed on a high-resistivity Si substrate. The heater of a resistor is placed at the center of the antenna and the thermistor together with an insulation layer between them is stacked. The electric lines are connected to the thermistor to flow bolometer current and the take the signal out from the thermistor. Only the bolometer cell comprising of the heater, the insulation layer and the thermistor is suspended on the air gap holed on the substrate. THz wave is irradiated from the back side of the surface on which the antenna is fabricated. This is because the ratio of substrate to air in the power emitted from a dipole antenna is proportional to $\epsilon'^{3/2}$ [26], and hence the antenna efficiency has the same dependence on ϵ' .

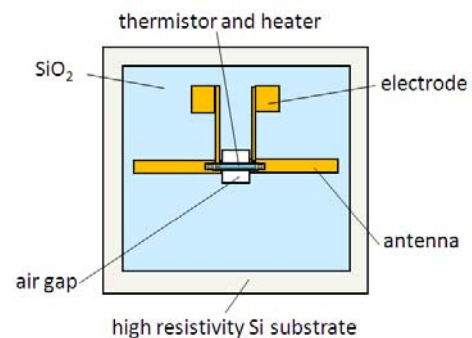


Fig. 1. Design of the THz Antenna-coupled Microbolometer (Bottom View)

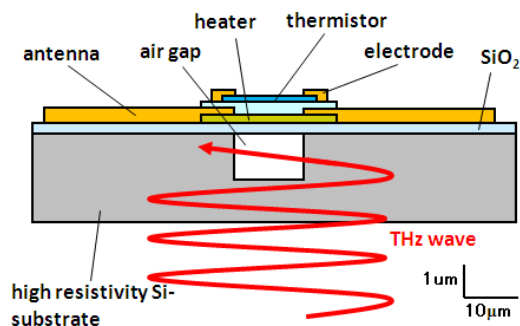


Fig. 2. Design of the THz Antenna-coupled Microbolometer (Side view)

This design has superior characteristics as following: (1) Thermal insulation is sustained only between a minute bolometer cell and an antenna on a substrate. (2) This structure brings the benefit of large and fast response in temperature change to rapid increase of THz radiation thorough small thermal capacitance of the bolometer cell. (3) Thermal conductance can be set reasonably small and DC responsivity and a time constant of response can be properly controlled by adjusting the size of bolometer cell though they are conflicting with each other. (4) An antenna load resistor can be determined independently from a thermistor resistor, which makes possible to optimize antenna-impedance and thermistor sensitivity. (5) Epi-structure of the microbolometer is simply deposited with materials used in Si process. Finally, (6) the process necessary for fabricating an air gap is not very difficult because the cavity is small.

3. Results and Discussion

Electromagnetic Simulations. The electromagnetic simulations of the half-wave antenna on a Si substrate are executed using Aether software of Field Precision LLC [27], based on there dimensional finite element method (3D-FEM), to examine the electromagnetic field emitted from the antenna and the induced current on the receiving antenna by the irradiated field, and also the HFSS software of ANSYS Inc. [28] is used to analyze impedance and resonance frequency of the antenna.

The antenna model used in the simulation is a half-wave antenna of gold (Au) placed on semi-infinite Si substrate with high-resistivity. Its length (L) and width (W) are $59.56 \mu\text{m}$ and $6 \mu\text{m}$ respectively: The former is determined from a resonant length L_r for 1 THz wave calculated by

$$L_r = \frac{0.48A}{\sqrt{\epsilon_e}} \lambda, \quad (1)$$

where $A = \frac{1}{1+W/L}$ [25]. The latter is set as small as

$1/10$ of L . Thickness of the antenna is $0.3 \mu\text{m}$, larger than the skin depth of Au at 1 THz.

Emitted field. The half-wave antenna on semi-infinite Si substrate is excited by 1 THz-RF current at its center and radiates electromagnetic wave, which electric fields are calculated by the electromagnetic simulation and displayed in Fig. 3. Fig. 4 shows the antenna patterns in the E-plane and the H-plane. These figures show the major power of electromagnetic wave is emitted into the Si substrate, which is consistent with the ratio $\epsilon'^{3/2}$ of substrate to air in the power radiated from a dipole antenna.

Induced current on the antenna. Current induced on the half-wave antenna on a Si-substrate irradiated by 1

THz wave from the substrate side is analyzed by the electromagnetic simulation. Figure 5 displays the current density on the half-wave antenna of all Au. This shows the feature of current is consistent with the theoretical distribution of $i(x) = i_m \cos(\pi x/L)$ as a

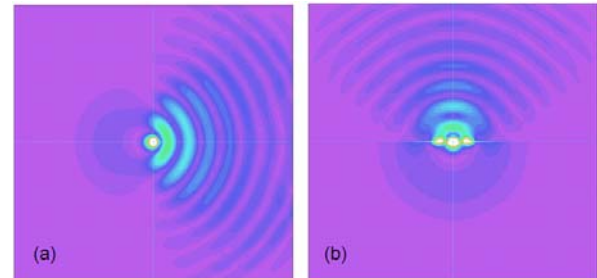


Fig. 3. (a) Electric Field Radiated from a Half-wave Antenna on a Si Substrate in the E-plane (Si Substrate is the Right Half). (b) Electric Field Radiated from a Half-wave Antenna on a Si Substrate in the H-plane (Si Substrate is the Upper Half)

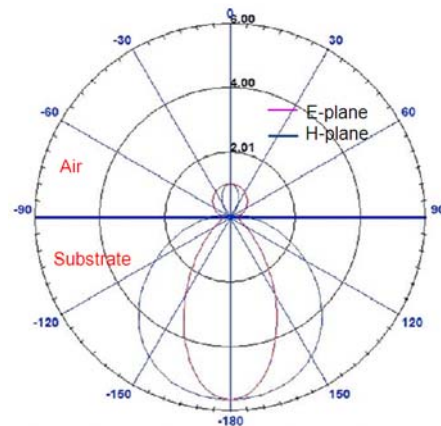


Fig. 4. Antenna Pattern of a Half-wave Antenna in the E-plane and the H-plane

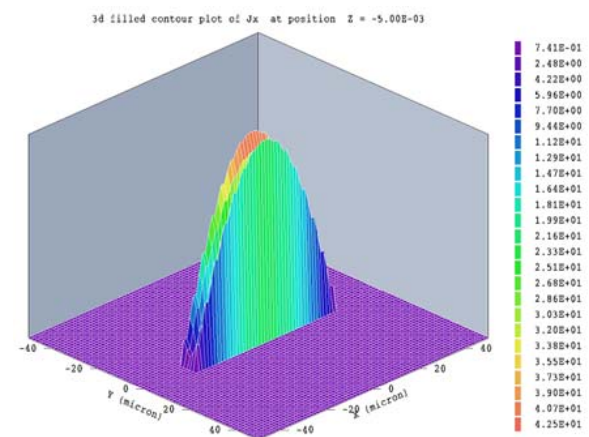


Fig. 5. Distribution of Current Density on the Half-wave Antenna of All Au

function of the position x along the antenna length, where i_m is the amplitude of current at the center.

If the half-wave antenna on a Si substrate has a gap of $10\ \mu\text{m}$ in length, the distribution of current density is disconnected at the gap as shown in Fig. 6. This situation is the same for the antenna with another size of gap. Therefore, the current doesn't flow over the gap in the Si substrate through change in dielectric polarization.

The current distribution is analyzed in Fig. 7, when a Ni:Cr line with the same width of $6\ \mu\text{m}$ as the Au antenna and a thickness of $0.1\ \mu\text{m}$ is placed on the $10\ \mu\text{m}$ gap and connecting to two parts of a half-wave antenna of Au on a Si substrate. This figure shows the current flows through the Ni:Cr line of higher resistivity with the same current density as on the Au antenna. Figure 8 displays the current distribution on the Ni:Cr line with $0.5\ \mu\text{m}$ width and $0.1\ \mu\text{m}$ thickness connecting

to the Au antenna, showing the current density on the narrow Ni:Cr line is much larger than on the Au antenna. These results mean the current flow is conserved at the boundary between Ni:Cr and Au. This is important for designing the resistance of heater connected to an antenna because the impedance matching between a heater and an antenna is not necessary. The resistances of the Ni:Cr lines with $6\ \mu\text{m}$ and $0.5\ \mu\text{m}$ widths are $6\ \Omega$ and $72\ \Omega$ respectively and these resistances can be adjusted almost freely to optimize the energy dissipation of the induced current and heat production.

Resonance frequency. Real and imaginary parts of impedance are shown in Fig. 9 as a function of frequency for a dipole antenna with a length of $49\ \mu\text{m}$ and a $10\ \mu\text{m}$ gap on a high-resistivity Si substrate, which is calculated through the electromagnetic simulation. The resonance frequency is extracted as a frequency at which the imaginary part of impedance

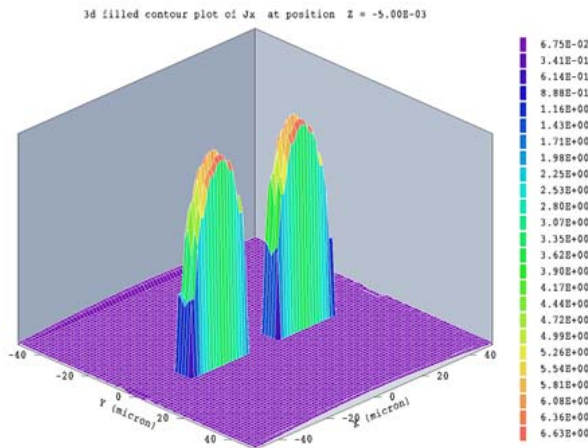


Fig. 6. Distribution of Current Density on the Half-wave Antenna of Au with a $10\ \mu\text{m}$ Gap at the Center

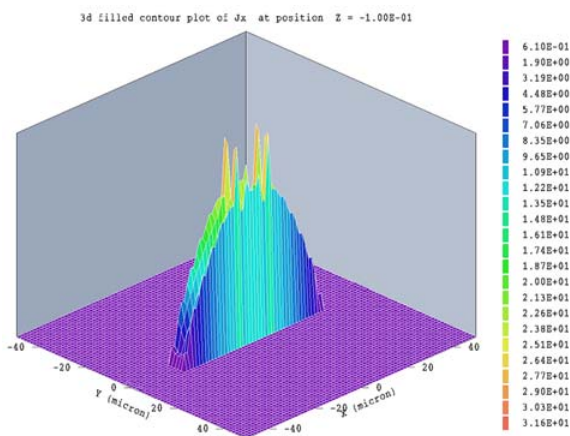


Fig. 7. Distribution of Current Density on the Half-wave Antenna of Au with a $10\ \mu\text{m}$ -long Gap, Connected by a Ni:Cr Line with $6\ \mu\text{m}$ Width and $0.1\ \mu\text{m}$ Thickness

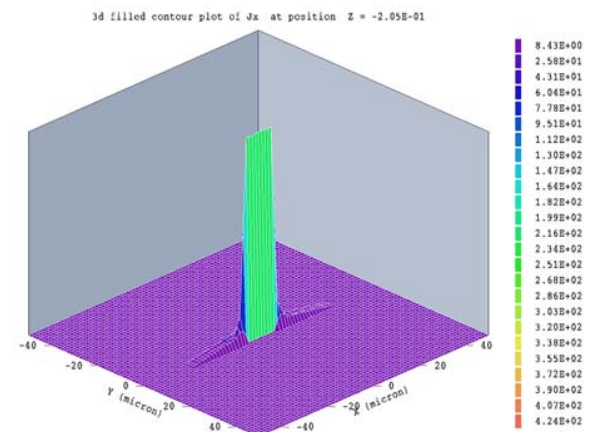


Fig. 8. Distribution of Current Density on the Half-wave Antenna of Au with a $10\ \mu\text{m}$ Gap, Connected by a Ni:Cr Line with $0.5\ \mu\text{m}$ Width and $0.1\ \mu\text{m}$ Thickness

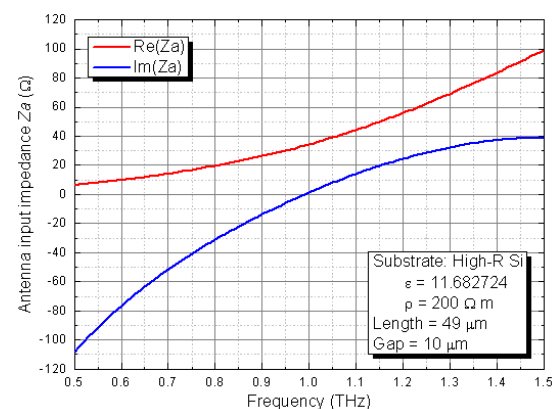


Fig. 9. Real and Imaginary Parts of Impedance as a Function of Frequency for a Dipole Antenna with a Length of $49\ \mu\text{m}$ and a $10\ \mu\text{m}$ Gap on a High-resistivity Si Substrate

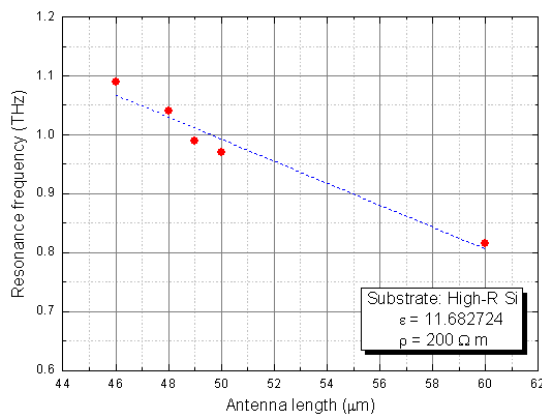


Fig. 10. Resonance Frequency of a Dipole Antenna on a High-resistivity Si Substrate as a Function of the Length of Antenna

(i.e. reactance) is zero, and hence it is about 1THz for the antenna with 49μm length and 10 μm gap. Resonance frequency of a dipole antenna on a Si substrate is displayed as a function of the length of antenna in Fig. 10. The length corresponding to the resonance frequency of 1 THz is about 49μm, which is shorter than the value from Eq. (1). This means a parameter A in Eq. (1) may be smaller than the approximate expression of $A=(1+W/L)^{-1}$.

4. Conclusions

High-performance THz detectors at room-temperature are important for various sensing applications of the THz wave, but even the best detectors in the present are far from the demand of the practical applications. Therefore, we propose and study an antenna-coupled microbolometer on a Si substrate to achieve a high-performance at a room-temperature for sensing at around 1 THz frequency where a infrared-type microbolometer with an absorption film is difficult to be developed. The structure of our detector is simple and convenient to design and easy to fabricate because only a small bolometer cell comprising of heater and thermistor is suspended on an air gap for thermal isolation. It also has potential to realize both high sensitivity and fast response by optimizing the design of the bolometer cell. The electromagnetic simulation demonstrates clearly the high antenna gain to the radiation from the substrate side. The current on an antenna induced by the THz irradiation flows on a heater placed at the center of the antenna, regardless of the heater resistance, meaning the impedance matching is not necessary between the antenna and the heater. Resistance of the heater in which the power almost equal to the available receiving power is as large as 73.13 Ω for a half-wave antenna. Irradiation powers absorbed by an antenna and an absorption film are basically the same if such condition as irradiated area

and polarization of radiation are almost equal. The antenna length corresponding to the resonance frequency of 1 THz is about 49 μm by the electromagnetic simulation, which is shorter than 56 μm from a simple analytical equation.

Acknowledgment

The authors acknowledge Prof. Hiroshi Inokawa, Assist. Prof. Hiroaki Sato and Dr. Tiwari Ajay of Shizuoka University for their collaboration on the research project of 1 THz room-temperature detector with high performance. The authors also acknowledge Dr. Kiyomi Sakai, the former Director of Special Laboratory, National Institute of Information and Communications Technology, and Emeritus Prof. Yoshizumi Yasuoka of National Defense Academy of Japan for their advice to the study on THz detectors and antennas. This study is partially supported by Industry-Academia Collaborative R&D from Japan Science and Technology Agency, JST.

References

- [1] K. Sakai (Ed.), Terahertz optoelectronics, Topics Appl. Phys. 97, Springer-Verlag, Berlin Heidelberg, 2005, p.350.
- [2] S.P. Mickan, X.-C. Zhang, Int. J. High Speed Elec. Sys. 13/2 (2003) 601.
- [3] R. Koehler, A. Tredicucci, F. Beltram, H.E. Beere, E.H. Linfield, A.G. Davies, D.A. Ritchie, R.C. Iotti, F. Rossi, Nature. 417 (2002) 156.
- [4] B.S. Williams, S. Kumar, H. Callebaut, Q. Hu, J.L. Reno, Appl. Phys. Lett. 83/11 (2003) 2124.
- [5] N. Karpowicz, H. Zhong, C. Zhang, K.-I Lin, J.-S. Hwang, J. Xu, X.-C. Zhang, Appl. Phys. Lett. 86/5 (2005) 054105.
- [6] K. Yamamoto, M. Yamaguchi, F. Miyamaru, M. Tani, M. Hangyo, Japan J. Appl. Phys. 43/3B (2004) L414.
- [7] H.-B. Liu, H. Zhong, N. Karpowicz, Y. Chen, X.-C. Cheng, Proc. IEEE 95/8 (2007) 1514.
- [8] K. Kawase, Y. Ogawa, Y. Watanabe, H. Inoue, Opt. Express. 11/20 (2003) 2549.
- [9] A.J. Fitzgerald, B.E. Cole, P.F. Taday, J. Pharm. Sci. 94/19 (2005) 177.
- [10] C. Joerdens, M. Koch, Opt. Eng. 47/3 (2008) 037003.
- [11] R.M. Woodward, B.E. Cole, V.P. Wallace, R.J. Pye, D.D. Arnone, E.H. Linfield, Michael Pepper, Phys. Med. Biol. 47 (2002) 3853.
- [12] M. Nagel, P.H. Bolivar, M. Brucherseifer, H. Kurz, A. Bosserhoff, R. Buttner, Appl. Phys. Lett. 80/1 (2002) 154.
- [13] N. S. Nishioka, P.L. Richards, D.P. Woody, Appl. Opt. 17 (1978) 1562.
- [14] P.R. Bratt, Semiconductors and Semimetals, vol. 12, In: R.K. Willardson, A.C. Beer (Eds.),

- Academic Press, New York, San Francisco, London, Chapter 2, 1977, p.482.
- [15] N. Hiromoto, M. Saito, H. Okuda, Jpn. J. Appl. Phys. 29 (1990) 1739.
- [16] A.G. Kazanskii, P.L. Richards, E.E. Haller, Appl. Phys. Lett. 31 (1977) 496.
- [17] N. Hiromoto, T. Itabe, H. Shibai, H. Matsuhara, T. Nakagawa, H. Okuda, Appl. Opt. 31 (1992) 460.
- [18] M. Aoki, S.R. Tripathi, M. Takeda, N. Hiromoto, Electron. Express. 9/5 (2012) 333.
- [19] D.P. Neikirk, W.W. Lam, D.B. Rutledge, Int. J. Infrared Millimeter Waves. 5/3 (1984) 245.
- [20] T. Uchida, K. Hayashi, T. Furuya, T. Tachiki, T. Idehara, Y. Yasuoka, The 33rd Int. Conf. Infrared Millimeter Terahertz Waves (IRMMW-THz 2008), Pasadena, CA, U.S.A., 2008.
- [21] F. Simoens, J. Lalanne-Dera, J. Meilhan, S. Pocas, D.T. Nguyen, J.-L. Ouvrier-Buffet, O. Cathabard, P. Gellie, S. Barbieri, The 36th Int. Conf. IR, MMW, and THz wavws (IRMMW-THz 2011), W2D.4, 2011.
- [22] C.M. Hanson, H.R. Beratan, R.A. Owen, M. Corbin, S. McKenney, Proceedings of SPIE Infrared Detectors: State of the Art. 1735. Ed. W. H. Makky, 1992, p.17.
- [23] R.A. Wood, C.J. Han, P.W. Kruse, Tech. Digest of IEEE Solid-State Sensor and Actuator Workshop, 1992, p.132.
- [24] N. Hiromoto, The 9th Takayanagi Kenjiro Memorial Symposium - 4th International Symposium on Nanovision Science, Nanospace Manipulation of Photon and Electrons for Nanovision Systems, (Hamamatsu Campus, Shizuoka Univ.), 30. Oct. 2007.
- [25] M. Konami, D.M. Pozar, D.H. Schaubert, IEEE Trans. Antenna Propagation, AP-33/6 (1985) 600.
- [26] D.B. Rutledge, D.P. Neikirk D.P. Kasilingam, In: Infrared and Millimeter Waves, vol. 10, K.J. Button (Ed.), Academic Press, New York, 1983, p.90.
- [27] Anon., Field Precision LLC, <http://www.fieldp.com>, 2011.
- [28] Anon., HFFS Industry Standard Enhanced, <http://www.ansys.com>, 2011